Journal of Hydrology: Regional Studies 38 (2021) 100971

Contents lists available at ScienceDirect

Journal of Hydrology: Regional Studies

journal homepage: www.elsevier.com/locate/ejrh

Assessment of dimension-reduction and grouping methods for catchment response time estimation in Hungary

Eszter D. Nagy [a,*], Jozsef Szilagyi [a,b], Peter Torma [a]

[a] Department of Hydraulic and Water Resources Engineering, Budapest University of Technology and Economics, Budapest, Hungary
[b] Conservation and Survey Division, School of Natural Resources, University of Nebraska-Lincoln, Lincoln, NE, USA

ARTICLE INFO

Keywords:
Catchment response time
Dimension reduction
Clustering
Catchment grouping
Empirical equation

ABSTRACT

Study region: 61 catchments located in Hungary, with drainage areas from 8.74 to 810 km^2.
Study focus: Many engineering tasks require the estimation of the catchment response time (T_r). The most frequently used T_r parameters are the time of concentration and the lag time. At ungauged catchments, they are usually estimated by empirical equations that relate T_r to catchment characteristics. This paper provides a comparative study of three dimension-reduction techniques and seven clustering methods for fitting empirical equations to the observed values of T_r. 60 catchment descriptors were calculated for each catchment, then three subsets with 1–3 descriptors were extracted from the entire parameter set during the dimension-reduction analysis. Two and four catchment groups were created during a cluster analysis, by re-calibrating the three equations that resulted from the dimension-reduction analysis.
New hydrological insights for the region under study: It is demonstrated that the principal component analysis can be easily outperformed by the linear correlation and the all-possible-regressions methods, the latter yielding a root-mean-squared error (RMSE) of 6.77 h when applied with three catchment descriptors. The most interesting finding of the dimension reduction is that T_r is strongly connected to field capacity in the region of study. The performance of the clustering methods varies considerably (RMSE = 5.05–12.03 h). The best overall performance comes from the residual approach (RMSE = 8.14 h on average). It is shown that several of the methods outperform the grouping based on geographical regions, however, the estimation error is reduced only in a few cases when compared to the regional estimation (i.e., one cluster) method. Clusters created based on catchment width yields the best results, resulting in RMSE values of 5.80 and 5.77 h (with two and four clusters, respectively). The comparison of the new and the existing empirical equations clearly demonstrated that the estimation of T_r needs improvement in Hungary, while the application of more than two clusters is unwarranted for the study region.

Abbreviations: T_r, catchment response time; T_c, time of concentration; T_L, lag time; T_p, time to peak; T_e, time to equilibrium; DMCA, detrending moving-average cross-correlation analysis; SRA, stepwise regression analysis; PCA, principal component analysis; PC, principal component; ECMWF, European Centre of Medium-Range Weather Forecast; CD, catchment descriptor; APR, all possible regressions; LCM, linear correlation matrix; RE, regional estimation; GC, geographical clustering; KM, k-means clustering; RT, regression tree; RA, residual approach; MC, Monte-Carlo; CDF, cumulative distribution function.

* Correspondence to: Muegyetem rakpart 3, 1111 Budapest, Hungary.
E-mail address: nagy.eszter@emk.bme.hu (E.D. Nagy).

https://doi.org/10.1016/j.ejrh.2021.100971
Received 29 June 2021; Received in revised form 17 November 2021; Accepted 19 November 2021
Available online 24 November 2021

1. Introduction

Estimating the response time of a catchment is a crucial step of many engineering tasks. Different time parameters need to be estimated for different purposes, such as peak flow estimation, modeling, or flood-risk/environmental hazard mapping. The most frequently used time parameters are the time of concentration (T_c), the lag time (T_L), the time to peak (T_p), and the time to equilibrium (T_e) (McCuen et al., 1987). The theoretical background of these time parameters is tangled, and their calculation is still an elaborate task, even though their study dates back more than 150 years. Recently, Beven (2020) highlighted the differences between T_c and T_e and how they became systematically mistreated in the last century. Moreover, several definitions are used for the calculation of time parameters in the literature, creating further confusion around their calculation. The present work aims to provide a broader picture of the catchment response time (T_r) in general.

Studies focusing on time parameter estimation involve three main assessment methods that rely on i) measured data; ii) hydraulic equations, and; iii) empirical or semi-empirical formulae. Measurements can be carried out using i) laboratory models; ii) a tracer substance, or; iii) registering rainfall and runoff data. Although tracer measurements provide detailed information on the runoff generation process and form the only approach that can be considered as a direct measurement of T_r, it can be completed only for research and not for an operational purpose (Pilgrim, 1976). The employment of model catchments built in a laboratory suffers from the same limitations. The ensuing results obtained by either of such measurements are not necessarily valid for natural catchments (Gaál et al., 2012).

The main disadvantage of applying measured time-series of rainfall and runoff is the lack of a clear definition for time parameters. However, for catchments larger than the experimental catchment size (i.e., a few square kilometers), it is the most effective way to collect information about the 'true' value of T_r since a large number of events on numerous catchments can be processed using historical precipitation and streamflow data. Recently, Giani et al. (2021) provided a new method to estimate the average value of the catchment response time using measured rainfall and runoff data. The authors of this paper used this method to calculate T_r on the event scale. These recent developments made the estimation of T_r from measured time-series more straightforward and comprehensive.

The observed value of T_r can be assessed by catchment descriptors to set up empirical equations. The performance of the equations can be bolstered in two steps: i) selecting catchment descriptors which describe the response variable (T_r) most efficiently, and; ii) through the grouping of catchments. The result of catchment grouping highly depends on the selection of descriptors. Therefore, identification of the proper catchment descriptors is a crucial step. There is a vast amount of parameters available in the literature. Ssegane et al. (2012) collected 72 topographic parameters, 66 climatic parameters, 98 soil parameters, and 15 land use/land cover parameters, while Sanborn and Bledsoe (2006) gathered 84 streamflow metrics from literature. Even if the set of examined parameters is reduced by hydrological reasoning at the very beginning, application of a dimension-reduction technique is typically required to set up a smaller parameter space.

The two most often used dimension-reduction techniques in hydrological studies are stepwise regression analysis (SRA) and principal component analysis (PCA). A notable difference between the two methods is that while SRA utilizes information from the response variable as it minimizes the prediction error, PCA would not necessarily involve the response variable (Ssegane et al., 2012). While PCA is helpful to reduce dimensions and group parameters, it may lead to the removal of hydrologically significant parameters. For example, Myronidis and Ivanova (2020) applied PCA to reduce the parameter space followed by employing SRA to estimate design flow values. As it turned out, it is not guaranteed that PCA would retain the most efficient parameter set in terms of design-flow estimation. Singh et al. (2009) also relied on PCA to group parameters and set up a reduced parameter set. They state that one parameter from each principal component (PC) can subsequently estimate specific hydrological processes. Even though this set of parameters indeed retains the largest information content from the initial parameter space regarding the variance, it is not guaranteed that the selected parameters will lead to the best estimation of the chosen hydrological process. Ssegane et al. (2012) compared SRA, PCA, and five other causal selection methods on parameter selection of known functional relationships. In their study, PCA was outperformed by SRA, and two of the causal selection methods performed the best.

Catchment grouping is a fundamental tool to transfer information from gauged catchments to ungauged sites. It can provide a deeper understanding of the underlying processes that control the studied runoff characteristics. Groups can be categorized based on their i) construction (fixed or targeted to the catchment of interest), and; ii) spatial continuity (contiguous or non-contiguous) (Blöschl et al., 2013). The applications of grouping methods may include the estimation of i) annual runoff; ii) seasonal runoff/flow regime; iii) flow duration curve; iv) low flow/design flow values, and; v) model parameters. Comprehensive studies usually focus on one application; however, different clustering techniques can easily lead to different results. Laaha and Blöschl (2006) found that employing seasonality regions based on low-flow exceedance yields the best result in the case of low-flow estimation. For flow duration curve estimation in France, the visual grouping method and the regression tree (RT) method performed equally well (Sauquet and Catalogne, 2011). Parajka et al. (2005) estimated the model parameters of a semi-distributed conceptual rainfall-runoff model the most successfully via a kriging approach and a donor catchment method based on similarity.

To the present authors' best knowledge, there is no literature available on grouping methods to estimate T_r. Ravazzani et al. (2019) examined the effect of catchment grouping on the performance of 24 empirical equations. However, their clustering approach was based on the result of flow duration curve estimation (Boscarello et al., 2016). They found that the predictions did not improve significantly when homogeneous groups of catchments were created.

The broad spectrum of such findings underlines the need for a comprehensive study of clustering methods concerning the estimation of T_r. An added motivation of the present study is that the currently employed equation for the estimation of T_c in Hungary dates back to 1958 (Wisnovszky, 1958), thus clearly requiring a revision. This paper focuses on two main aspects: i) to find the optimal

dimension-reduction method, and; ii) to identify the best catchment-grouping approach, along with the optimal number of groups. We also focus on quantifying the PCA's effectiveness as a parameter selection technique (and conclude that it does not necessarily yield the best set of parameters), and on assessing the improvement via comparison to existing empirical equations. A further novelty of the present study is that we provide the clustering methods' efficiency in terms of probability by a Monte-Carlo approach.

2. Study area and data

This study involves 61 small- to medium-sized catchments located in the Carpathian Basin. An overview of the catchments' location is provided in Fig. 1, while Table 1 lists some important characteristics. The size of the catchments ranges from 8.74 to 810 km^2, while the average catchment area is 206 km^2. 6.5% of the catchments are larger than 500 km^2, and 54% of the catchments have an area smaller than 150 km^2. The proportion of forested area ranges from 3.83% to 88.7%, while the impervious area is between 0.275% and 19.9%, based on the Copernicus land-use/land cover products (Copernicus, 2020a, 2020b). The soil types covering the catchments are dominantly deposits, such as glacial and alluvial, loess and loess-like, tertiary, and older deposits. Third of the catchments coincide with karst regions, while volcanic rocks, such as andesite, rhyolite, and basalt are dominant in a few (<5%) ones. Sandstone, shale, and phyllite are dominantly present in even fewer catchments. The study covers the years from 2000 to 2017 when the annual rainfall and runoff ranged between 394 and 1377 and 21.1–642 mm, respectively. The region's climate is predominantly warm-summer humid continental (Dfb), based on the Köppen climate classification (Peel et al., 2007), while the aridity index (i.e., the annual potential evaporation divided by the annual precipitation) varies between 0.75 and 1.25.

Catchment delineation was performed by the Copernicus Land Monitoring Services' EU-DEM v1.1 digital surface model. This is a freely available dataset with a spatial resolution of 25 m in raster format (Copernicus, 2016). Three main selection criteria were applied regarding the selection of the discharge time-series, namely i) no significant human influence on flow; ii) high temporal resolution of measurements, and; iii) record availability for at least ten years (similar to Sauquet and Catalogne, 2011). The local Water Directorates provided high-resolution (5 min) discharge and precipitation time-series for 61 and 17 stations, respectively. Since not every catchment has a nearby rainfall gauging station, the European Centre of Medium-Range Weather Forecast (ECMWF) reanalysis data from the Copernicus Climate Data Store were used in addition to the gauging station data. The used product is the Era5 Land dataset (Copernicus, 2019), with an hourly temporal and a 0.1° x 0.1° (~7.5 km x 11 km) spatial resolution. The applicability of the ECMWF reanalysis data to response time calculation was examined separately in a previous study (Nagy and Szilágyi, 2020). In the referred study, eight different graphical T_r definitions were compared at the 38 catchments having both gauging station and ECMWF precipitation data. We found that the ECMWF data is adequate for T_r estimation, especially when the centers of masses and peaks of the measured runoff and rainfall time-series are used.

3. Methodology

3.1. Overview

The methodology of the study is comprised of three main steps: i) assembling the initial data which included calculation of the observed T_r values and evaluation of the catchment descriptors (CDs); ii) reduction of the initial CD dataset into different number of CDs by various dimension-reduction methods, and; iii) grouping catchments into different number of groups by selected clustering methods. The first step resulted in one characteristic, i.e., the observed value of T_r for 61 watersheds each, accompanied by 60 CDs for each catchment. The second step yielded the optimal subsets of CDs by applying three dimension-reduction methods. Lastly, the most efficient combination of the number of groups and clustering method was identified through cluster analysis. The general form of the

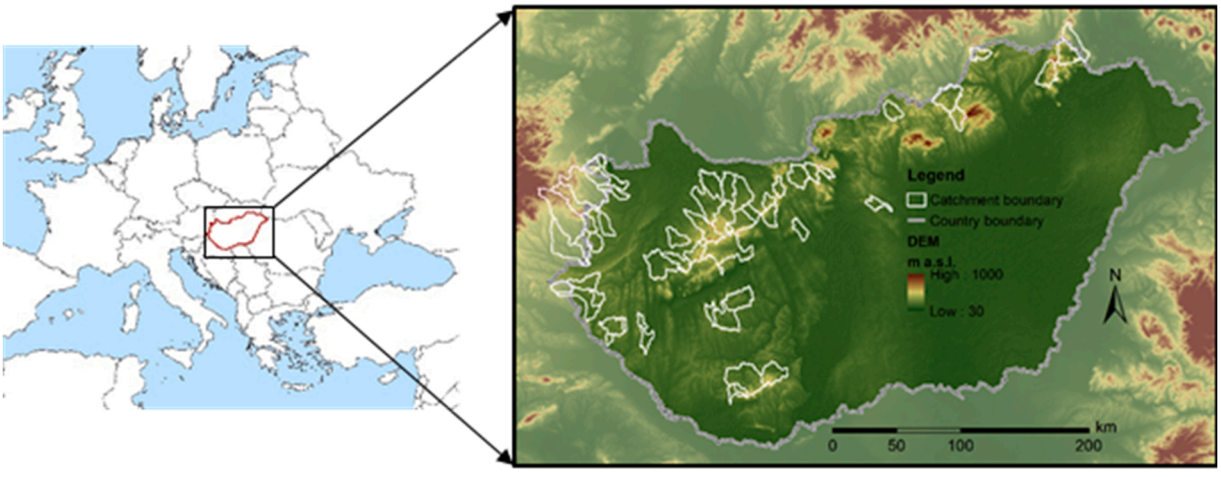

Fig. 1. Overview of the study area and catchments.

Table 1
Minimum, maximum, and average values of the important catchment descriptors.

	Catchment area [km^2]	Longest flowpath [km]	Elevation [m a.s.l.]	Average slope of watershed [%]	Highest stream order (Strahler) [-]	Ratio of impervious surfaces [%]	Ratio of forests [%]	Annual runoff [mm]	Annual precipitation [mm]	Aridity index [-]
Minimum	8.74	5.08	103	1.05	2	0.275	3.83	21.1	394	0.75
Maximum	810	88.3	1629	22.2	5	19.9	88.7	642	1377	1.25
Average	206	32.9	264	9.69	4	8.89	69.4	74.6	756	1.10

fitted empirical equations throughout the study is given as

$$T_{r,mod} = \alpha_1 \bullet X_1^{\alpha_2} \bullet X_2^{\alpha_3} \bullet \cdots \bullet X_n^{\alpha_{n+1}} \quad (1)$$

where $X_1, \ldots, X_n$ are the selected CDs, $\alpha_1, \ldots, \alpha_{n+1}$ are model coefficients, while the number of selected parameters (n) can be 1 through 3. The overview of the workflow and the applied methods are summarized in Fig. 2.

3.2. Derivation of T_r from observations

The characteristic, measured values of T_r were calculated for each catchment applying the detrending moving-average cross-correlation analysis (DMCA) following Giani et al. (2021). The strength of the DMCA method is that it can find the timescale at which two time-series are linked even when they exhibit different frequency spectra and are nonlinearly related (Giani et al., 2021). Therefore, the DMCA method is capable to estimate T_r using the measured precipitation and discharge time-series. This method can determine T_r values for every event, resulting in a set of T_r values for each catchment. For the 61 examined catchments, 11,646 event-based values were collected altogether. The number of events (i.e., T_r values) per catchment ranged from 25 to 625 with a median of 117.

In what follows, the median of the DMCA-based set of values is considered as the characteristic, observed value of T_r for each catchment, hence, the empirical equations later were fitted using these values. In Fig. 3, we present the distribution of the observed T_r values by means of boxplots, representing the medians, the 25th and 75th percentiles, and the outliers, along with a map of the observed median values.

From Fig. 3 it is clear that the value of T_r exhibits significant variability, especially for larger catchments. This can be attributed to the fact that the distribution of rainfall becomes less uniform as the catchment area increases. The authors would prefer to consider T_r as a stochastic value, since its value is exposed to randomness, e.g., the distribution of precipitation over a catchment. However, in this

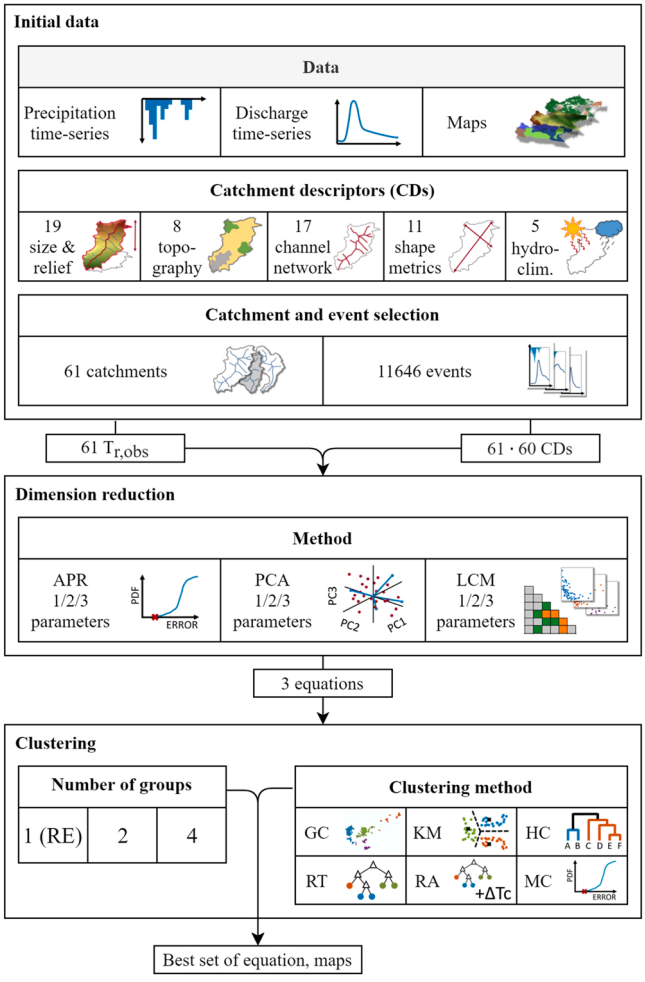

Fig. 2. Workflow of the study.

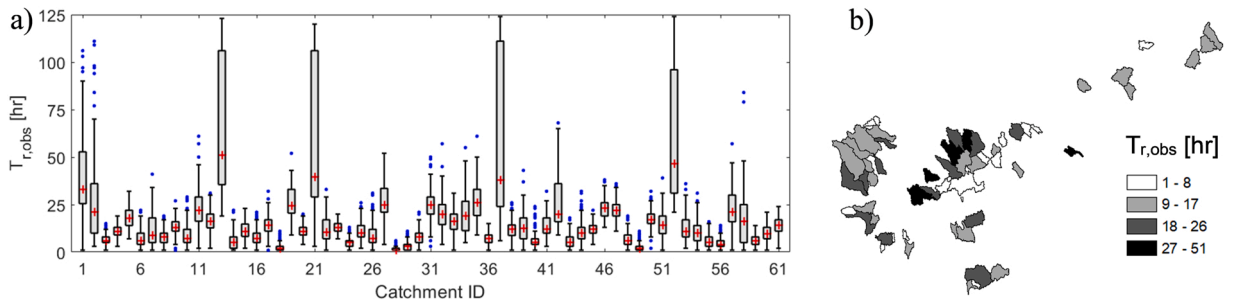

Fig. 3. a) Observed values of T_r [hr] resulting from the DMCA-based event selection method. Red crosses denote the characteristic T_r values for each catchment as the median of the observed set of values. b) Spatial distribution of the observed, characteristic values of T_r.

study we only aim to estimate the median of the measured set of T_r values. This median can be interpreted as the T_r of a "typical flood".

3.3. Catchment descriptors

Since the aim is to connect the observed value of T_r to CDs, altogether, 60 parameters were collected and classified into five main categories: i) size and relief; ii) topography; iii) channel network; iv) shape indices, and; v) hydro-climatological indices. The list of parameters and their definitions can be found in Appendix A1-A5, including name, abbreviation, and measurement unit, along with a reference. A selection of CDs is presented in Fig. 4.

3.4. Dimension-reduction

The initial number of CDs had to be reduced to a smaller parameter set which could subsequently be used to construct and fit empirical equations to the observed values of T_r. First, the method of all possible regressions (APR) were evaluated, which means the evaluation of all possible parameter combinations by Eq. (1) (see above in Section 3.1). The number of combinations grows from 60 to 1830 and 35990, as the number of CDs increases from one to two and three, respectively. This method's output should agree with the result of SRA in moderately well-behaved problems (Hocking, 1976), although Gugel (1972) reported 37% improvement in the results when APR was compared to SRA. The efficiency of other dimension-reduction methods can be assessed in probability terms since APR yields the probability distribution function of the performance index. As a second dimension-reduction technique, PCA was employed, and one parameter with the highest load on the first three PCs was kept. The third method was simple but arbitrary to a certain degree. The parameter sets were obtained from the linear correlation matrix (LCM) between the response variable (T_r) and the entire CD set. Parameters expressing the highest correlation with T_r but producing a weak correlation (Pearson correlation coefficient, $r < 0.7$) among each other were selected. According to previous studies on empirical T_r estimation equations (Azizian, 2018; Fang et al., 2008;

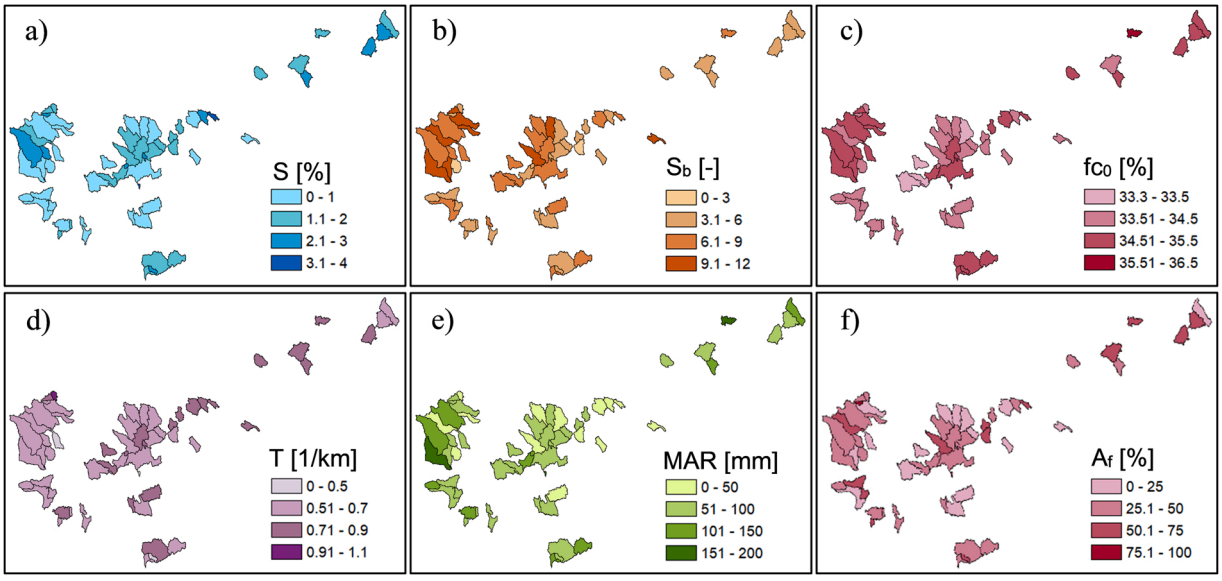

Fig. 4. Maps of different CDs: a) slope of the longest flow path (S [%]); b) basin shape factor (S_b [-]); c) field capacity at the soil surface (fc_0 [%]); d) drainage texture (T [1/km]); e) mean annual runoff (MAR [mm]); f) forested area (A_f [%]).

Grimaldi et al., 2012; Nagy et al., 2016; Ravazzani et al., 2019), most equations include one to three parameters. Additionally, the selection of four or more CDs would have increased the computation time of the APR method significantly, since the number of possible CD combinations grows an order of magnitude with each additional CD. Therefore, with the help of these dimension-reduction methods (APR, PCA, and LCM), one to three parameters were selected out of the 60 CDs.

3.5. Catchment grouping

Altogether, seven clustering methods were compared: regional estimation (RE), geographic clustering (GC), k-means clustering (KM), hierarchical clustering (HC), regression tree (RT) method, residual approach (RA), and Monte-Carlo (MC) approach. RE means no clustering (or one cluster); its inclusion is meant to show the efficiency of applying different numbers of clusters. In the following, the array of estimated T_r values comprises the dependent or response variable, while the independent variables are the selected CDs using the three dimension-reduction methods (APR, PCA, and LCM). The above clustering methods are widely used; here, we only present a short description of each method.

GC is based on the regions defined in the most recent design estimation manual, published by the General Directorate of Water Management (General Directorate of Water Management, 2001). The manual differentiates six regions as 'well distinguishable runoff regions in Hungary', but it gives no further explanation on the creation of such units. It is therefore assumed that the regions were created with the help of geological and hydrological (i.e. catchment) boundaries, referred to as geographical units. The six regions presented in the manual were later merged into four and two separate groups. The groups were created with consideration to the geological and climatological properties of the Carpathian Basin. The original and the merged groups are presented in Fig. 5.

KM was performed by Lloyd's algorithm (Lloyd, 1982) which does not include the response variable and consists of the following steps: i) choosing the initial cluster centers (or centroids) randomly from the data points; ii) computing point-to-cluster-centroid distances of all residual points to each centroid based on the chosen distance metric; iii) assigning each point to the cluster with the closest centroid; iv) computing the average of the points in each cluster to obtain new centroid locations; v) repeating steps ii)-iv) until cluster assignments stop changing; vi) repeating i)-v) until the number of replicates is reached. The number of replicates defines the number of repetitions of the clustering procedure starting from the random selection of initial cluster centers. This method minimizes the total variance of clusters, which is the sum of the deviation of each data point from its cluster's center by the chosen distance metric. The latter meant the sample correlation between the data points (treated as sequences of values) when subtracted from unity. Each centroid is the component-wise mean of the points in that cluster, after centering and normalizing those points to zero mean and unity standard deviation. The algorithm has two parameters: the maximum number of iterations and the number of replicates which were set to 10,000 and 100 respectively, in order to ensure a global optimum. The main disadvantage of this method is that the number of clusters must be defined before applying the algorithm. More detailed information on KM is given by Everitt et al. (2011) in Chapters 5.4.1–5.4.3.

HC, in contrast, does not require the number of clusters defined since it builds a dendrogram based on data point distances (Everitt et al., 2011). The dataset can be split at the desired level into clusters using the dendrogram. The correlation method was chosen again as the distance metric. This algorithm maximizes the distances between the clusters. Its advantage is the visualization of the clusters since outliers can be easily spotted on the dendrogram.

The RT method creates a decision tree with the desired number of nodes and bins (Breiman et al., 1984). The bins represent the clusters ensuring their maximum homogeneity. This method's advantage is that it needs no parametrization and is sensitive to outliers (Laaha and Blöschl, 2006). However, it results in one discrete value of the response variable for each cluster.

The RA involves applying the RT method using the residuals ($T_{r,res}$) of the response variable's regional estimation. Hence, the residual becomes the response variable, and one CD is used as the independent variable to define the clusters (bins). The residual is simply calculated as $T_{r,res} = T_{r,mod} - T_{r,obs}$, where $T_{r,mod}$ is the modeled while $T_{r,obs}$ is the observed value of T_r. Every CD was tested as the independent variable. On average, drainage texture (T [1/km]) performed the best; therefore, it was used for every set of CDs and every number of groups.

The MC approach aims to find the optimal set of clusters by testing a high number (100,000) of sets. First, the number of catchments in each cluster was defined randomly. The minimum number of catchments was set to $n + 2$, were n is the number of CDs involved in the empirical equation (see Section 3.1) to ensure the stability of the fitted regression. The maximum number of catchments were set to $61 - (k - 1) \bullet (n + 2)$, where k is the number of clusters. This way, the minimum number of catchments can be selected for each cluster. Second, the required number of catchments were selected, also on a random basis. This approach yields the cumulative distribution

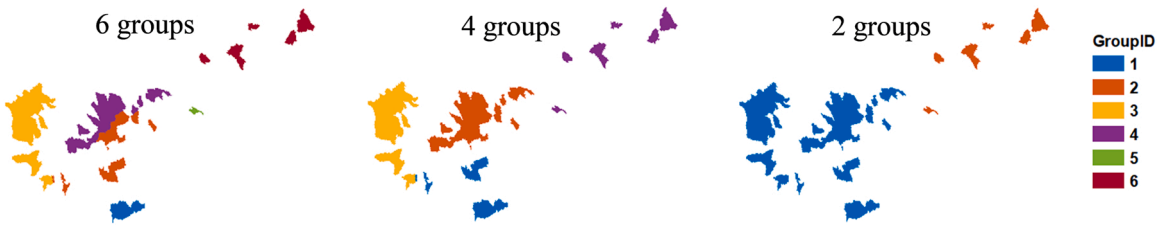

Fig. 5. Geographical grouping by the General Directorate of Water Management (left), with a subsequent merger into four and two separate groups (middle and right) in this study.

function (CDF) of the performance indices. Therefore, the performance of the other clustering methods can be assessed in terms of probability. Even though the optimal set of clusters can be found, this is the only method where ungauged catchments could not be sorted into clusters based on their CDs.

3.6. Goodness-of-fit measures

During the dimension reduction analysis, the following goodness-of-fit measures were used: Pearson correlation coefficient (r [-]), Nash-Sutcliffe efficiency (*NSE* [-]) (Nash and Sutcliffe, 1970), root-mean-squared error (*RMSE* [hr]), Akaike information criteria (*AIC* [-]) (Fox, 2016), and the sum of relative differences (ΔT_r [%]). These were calculated as:

$$r = \frac{\sum_{i=1}^{N}(x_i-\bar{x})(y_i-\bar{y})}{\sqrt{\sum_{i=1}^{N}(x_i-\bar{x})^2\sum_{i=1}^{N}(y_i-\bar{y})^2}} \tag{2}$$

$$NSE = 1-\frac{\sum_{i=1}^{N}(y_i-x_i)^2}{\sum_{i=1}^{N}(x_i-\bar{x})^2} \tag{3}$$

$$RMSE = \sqrt{\frac{\sum_{i=1}^{N}(y_i-x_i)^2}{N}} \tag{4}$$

$$AIC = N\bullet\ln\left(\mathrm{RMSE}^2\right)+2\bullet(\mathrm{n}+1) \tag{5}$$

$$\Delta T_r = \frac{\sum_{i=1}^{N}|y_i-x_i|}{\sum_{i=1}^{N}x_i}100 \tag{6}$$

where x_i is the observed value ($T_{r,obs}$), y_i is the modeled value ($T_{r,mod}$), n is the number of model parameters (CDs) and N is the number of observations. The value of r can range from −1–1, meaning perfect inverse linear and linear relationships, respectively, at its extremes. The value of *NSE* demonstrates the model's capability of giving a better estimation than the mean of the observed values, and its value can range from -∞ to 1. If *NSE* is in the range of 0–1, the model provides a better estimation than the observed values' mean. An *NSE* value of 1 represents a perfect fit of the model. The *RMSE* value is 0 for a perfect fit, and the smaller the value the better the model. The value of *AIC* can quantify the relative information loss/gain of the models: a higher value denotes a more efficient equation. The value of ΔT_r defines the model's estimation error in percentage relative to the observed values. All measures were employed during the dimension-reduction analysis, while only *RMSE* and *NSE* were used for the cluster analysis.

3.7. Existing empirical equations

As mentioned in Section 1, the empirical equation for T_r estimation dates back to 1958 in Hungary (Wisnovszky, 1958). Many other countries/regions developed their own empirical equations, therefore a large amount of equations can be found in the literature. Also, there are numerous studies comparing different empirical equations and assessing their performances (e.g., Azizian, 2018; Kaufmann de Almeida et al., 2017; Nagy et al., 2016; Michailidi et al., 2018; Perdikaris et al., 2018; Ravazzani et al., 2019). In order to express the improvement in the estimation accuracy, four existing empirical equations were applied to estimate T_r. We chose to use the Wisnovszky, Salcher, Ventura, and Haktanir-Shezen equations. The first is the most often used equation in Hungary, and it was derived from the Salcher equation. The Ventura equation is also mentioned in one of the Hungarian textbooks. The Haktanir-Shezen equation was chosen based on the results of a former study (Nagy et al., 2016). The equations and their performance indices (*RMSE* and *NSE*) are presented in Table 2.

Table 2
The existing empirical equations and their performance indices. In the equations, L [km] is the longest flow path, A [km^2] is the catchment area, S [%] is the slope of the longest flow path, and L_{max} [km] is the length of the main stream (for more details see Appendix A1 and A3).

Name and reference	Equation	*RMSE* [hr]	*NSE* [-]
Wisnovszky (1958)	$T_c = \frac{L^2}{\sqrt{A}\bullet S/100}$	13.6	-0.680
Salcher (Wisnovszky, 1958)	$T_c = \frac{1}{600}\bullet\frac{\mathrm{L}}{\sqrt{\mathrm{S}/100}}$	10.5	0.00508
Ventura (Kaufmann de Almeida et al., 2017)	$T_c = 0.1272\bullet\sqrt{\frac{\mathrm{A}}{\mathrm{S}/100}}$	11.3	-0.169
Haktanir and Sezen (1990)	$T_c = 0.7473\bullet \mathrm{L}_{\mathrm{max}}^{0.841}$	9.31	0.210

4. Results

4.1. Dimension-reduction

One to three CDs were identified applying PCA, LCM, and APR. Eq. (1) was fitted using these CDs in each case. The model coefficients in Eq. (1) were estimated by ordinary least squares. The model performance was assessed by executing leave-one-out cross-validation, consisting of the following steps: i) remove catchment *j* from the dataset; ii) estimate the coefficients of the equation using all (*N*-1) catchments without catchment *j*; iii) apply the fitted equation to estimate the value of T_r at catchment *j* ($T_{r,mod,j}$); iv) repeat steps i)-iii) for all *N* catchments; v) calculate the goodness-of-fit measures (*r*, *NSE*, *RMSE*, *AIC*, ΔT_r). As a result, one equation for each dimension-reduction technique was selected and used afterward during the evaluation of the clustering techniques.

PCA showed that the first three PCs explain 26.7%, 14.3%, and 10.2% (51.2% altogether) of the total variance of the dataset. The CDs having the highest loads on the PCs are *P* (basin perimeter), H_{max} (maximum elevation), and R_c (elongation ratio). Two of these CDs (*P* and H_{max}) belong to the size and relief category, while R_c is a shape index. The CDs having the highest loads on the following three PCs are *MAP* (mean annual precipitation), C_m (channel maintenance), and ks_0 (saturated hydraulic conductivity). These CDs are part of the hydro-climatological indices, channel network parameters, and size and topography metrics, respectively. This underlies

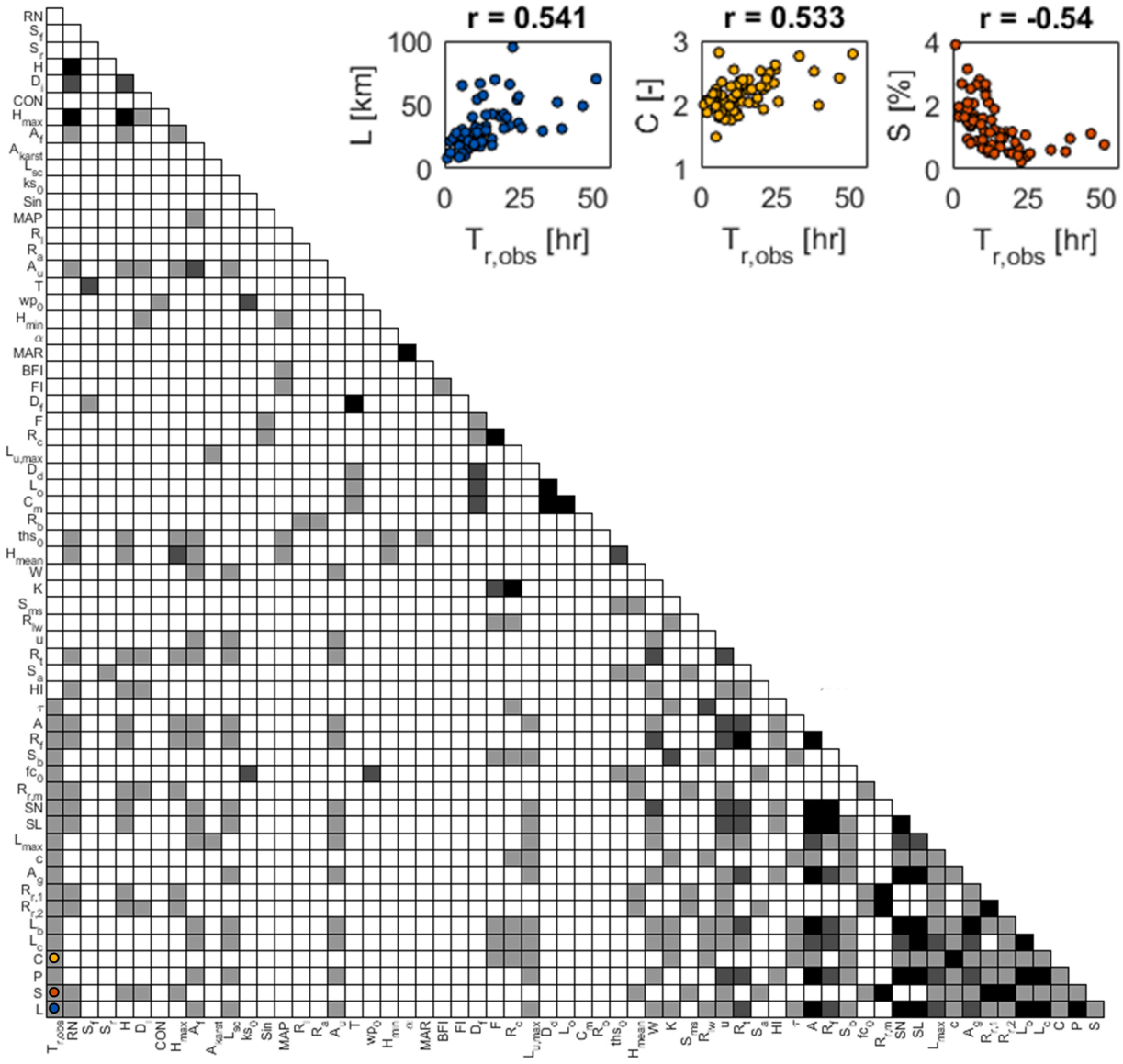

Fig. 6. Linear correlation matrix of the CDs (black: $r \geq 0.9$, dark grey: $0.9 > r \geq 0.7$, light grey: $0.7 > r \geq 0.4$, white: $0.4 > r$) and scatterplots of CDs and T_r with the strongest correlations.

the efficiency of PCA retaining the highest variability of the initial dataset since the resulting CDs do not belong into only one or two descriptor categories.

The LCM method resulted in the correlation matrix of the CDs and T_r (Fig. 6). The CDs selected with this method are L (longest flow path), S (slope of longest flow path), and C (compactness). These parameters describe size, relief, and shape. L is strongly ($r \geq 0.9$) correlated with SL, SN, A, P, L_b, and L_c, while S is strongly correlated with other relief metrics ($R_{r,1}$, $R_{r,2}$ and $R_{r,m}$). The latter is expected since their formulas are based on the ratio of the relief (H) and other strongly correlated CDs (L, P, L_b, $A^{1/2}$). C is strongly correlated with c (circularity) because a functional relationship exists between these two metrics, namely $c = 1/C^2$. The linear correlation matrix did not reveal any unexpected strong correlation amongst the CDs. It can also be seen that in some cases the correlation is not linear in nature (Fig. 6), which underlies the need for non-linear analyses, such as APR.

The results of APR (i.e., empirical distribution functions) can be seen in Fig. 7, along with the performance of the other two (PCA and LCM) dimension reduction methods for r, NSE, $RMSE$, ΔT_r, and by the number (1, 2, or 3) of CD values prescribed. Table 3 displays the fitted T_r equations and their performance metrics (for r, NSE, $RMSE$, AIC, and ΔT_r). The coefficient values in the equations are the means of the values resulting from the cross-validation process.

As expected, APR provided the lowest estimation error with an $RMSE$ of 6.77 h and an NSE value of 0.583, employing three CDs. The LCM dimension reduction method outperformed PCA at every number of CDs. Increasing the number of CDs in the equations did not significantly reduce the prediction error in the case of PCA. In terms of probability, PCA and LCM identified CDs performing in the upper 20%. The value of NSE is negative for 39%, 18%, and 10% of the combinations when applying 1, 2, and 3 CDs, respectively. ΔT_r varies from 34.6% to 43.8%, while r changes between 0.480 and 0.764.

The AIC value of the best set of CDs does not change considerably when increasing the number of CDs from 2 to 3. The difference is more significant in the case of the LCM equations, while the variation in the performance is almost negligible considering the PCA equations. In what follows, the three-parameter versions of the equations were used to make the cluster analysis results more comparable. The CDs of these equations (see Table 3) were applied subsequently during the cluster analysis when the equations' coefficients were recalculated for the clusters. The coefficients remained the same for the RE method as displayed in Table 3 since RE only consists of one cluster.

4.2. Catchment grouping

The general form of the fitted equation remained the same as in the case of the dimension-reduction (see Eq. 1), and the leave-one-out cross-validation was again performed (Laaha and Blöschl, 2006) as follows: i) remove catchment j from the dataset; ii) update the catchment grouping for the remaining N-1 catchments; iii) assign catchment j to one of the groups obtained in step ii); iv) estimate the coefficients of the equation using all (N-1) catchments apart from catchment j; v) apply the fitted equation to estimate the value of T_r at catchment j ($T_{r,mod,j}$); vi) repeat step i)-v) for all N catchments; vii) calculate the goodness-of-fit measures ($RMSE$ and NSE). The final values of model coefficients can be assessed as the means of the model parameters calculated for the groups. In total, 111 equations were fitted, applying the seven clustering methods and creating two and four groups to fit the empirical functions employing the CDs determined by the three dimension-reduction methods. We created only one cluster applying the RE method which yielded only 3 equations, while the other 6 clustering methods result in $(2 + 4) \times 3$ equations each. So, we obtain $3 + 6 \times (2 + 4) \times 3 = 111$ equations.

The CDFs of the performance indices ($RMSE$ and NSE) resulted from the MC method, and the performance of the other clustering methods are presented in Fig. 8 and Table 4. The CDFs flatten as the number of groups increases from two to four. This is because, as the number of clusters increases, the number of catchments within a group decreases. Since the calibrated function is a power function, its sensitivity to extrapolation is relatively high. The model parameters are more stable when they are calibrated for a higher number of catchments.

The MC approach clearly shows that the performance can be improved by at least 20% finding the right groups, but there is no unequivocal method that yields better results than RE. RA is able to find more efficient groups in some cases but does not improve the performance of the equations significantly. Also, it cannot be assured that using drainage texture (T) for RA as the independent variable

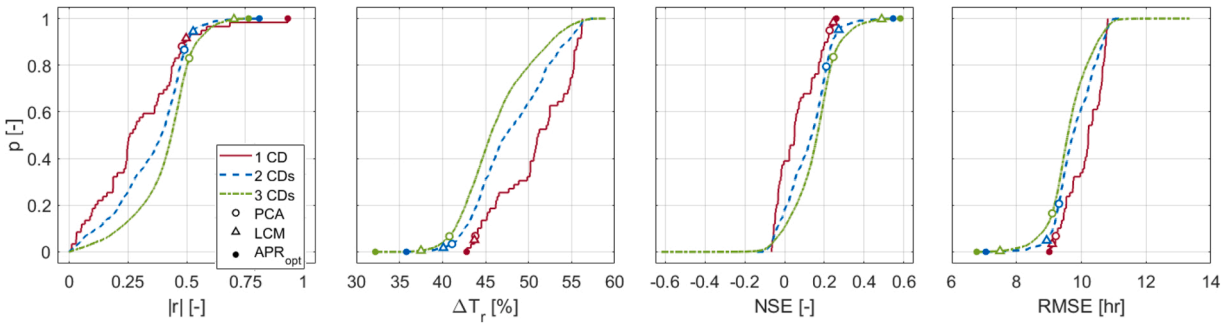

Fig. 7. Cumulative distribution functions of $|r|$, NSE, $RMSE$, and ΔT_r from APR (lines), along with the PCA and LCM performances for the prescribed number (1, 2, or 3) of CDs (markers).

Table 3
Goodness-of-fit measures and their exceedance probability (p [%], the probability that a better relationship exists) of the different dimension-reduction methods and CD sets (CDs in the framed equations were used for the cluster analysis).

Method	Number of CDs	r Value [-]	r p [%]	ΔT_r Value [%]	ΔT_r p [%]	*NSE* Value [-]	*NSE* p [%]	*RMSE* Value [hr]	*RMSE* p [%]	*AIC* [-]	Equation
PCA	1	0.480	11.9	43.8	6.78	0.227	5.08	9.21	6.78	269	$T_r = 0.50 \cdot P^{0.73}$
	2	0.490	13.4	41.1	3.39	0.210	20.57	9.31	20.63	265	$T_r = 5.44 \cdot \frac{P^{0.83}}{H_{max\{fc\}}^{0.46}}$
	3	0.511	17	40.8	6.67	0.246	16.5	9.10	16.5	265	$T_r = 6.40 \cdot \frac{P^{0.72}}{H_{max\{fc\}}^{0.43} \cdot R_c^{0.46}}$
LCM	1	0.498	8.47	43.7	5.08	0.246	1.69	9.10	3.39	268	$T_r = 1.33 \cdot L^{0.70}$
	2	0.528	5.60	40.1	1.69	0.273	4.85	8.93	4.91	264	$T_r = 2.95 \cdot \frac{L^{0.47}}{S^{0.30}}$
	3	0.702	0.3	37.5	0.54	0.489	0.31	7.49	0.31	238	$T_r = 1.70 \cdot \frac{L^{0.30} \cdot C^{1.45}}{S^{0.25}}$
APR	1	0.931	0	42.8	0	0.261	0	9.01	0	266	$T_r = 2.50 \cdot A_g^{0.40}$
	2	0.810	0	35.8	0	0.547	0	7.05	0	236	$T_r = 48.8 \cdot \frac{L^{0.84}}{(fc_0 \cdot 100 - 30)^{2.84}}$
	3	0.764	0	32.2	0	0.583	0	6.77	0	233	$T_r = 48.7 \cdot \frac{A_g^{0.27} \cdot S_b^{0.72}}{(fc_0 \cdot 100 - 30)^{2.57}}$

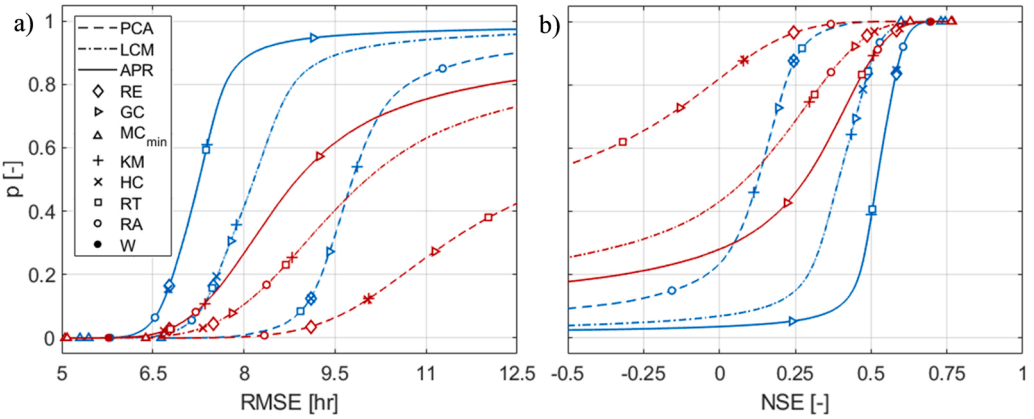

Fig. 8. Results of the different clustering methods. CDFs of a) *RMSE* and b) *NSE* resulting from the MC approach and three dimension-reduction methods (PCA, LCM, APR) creating two (blue) and four (red) groups, along with the goodness-of-fit measures of the different clustering techniques.

Table 4
Estimation errors (*RMSE* and *NSE*) of the seven clustering and three dimension-reduction methods for the different number of catchment groups.

	PCA	LCM	APR	PCA	LCM	APR	PCA	LCM	APR	PCA	LCM	APR
	RMSE [hr]						*NSE* [-]					
RE	9.10	7.50	6.77	9.10	7.50	6.77	0.25	0.49	0.58	0.25	0.49	0.58
	Two groups			Four groups			Two groups			Four groups		
GC	9.41	7.78	9.14	11.14	7.80	9.24	0.19	0.45	0.24	-0.13	0.45	0.22
MC_{min}	7.53	5.44	5.30	6.38	5.05	5.09	0.60	0.73	0.74	0.63	0.77	0.76
KM	9.86	7.88	7.41	10.06	8.79	7.35	0.11	0.43	0.50	0.08	0.30	0.51
HC	9.10	7.55	6.75	10.04	7.32	6.69	0.25	0.47	0.58	0.08	0.51	0.59
RT	8.94	7.48	7.38	12.03	8.68	6.79	0.27	0.49	0.50	-0.32	0.31	0.47
RA	11.27	7.14	6.53	8.34	8.37	7.21	-0.16	0.53	0.61	0.37	0.37	0.52

would lead to similar results for other catchments with different properties. It is hard to create an order for the different clustering methods in terms of performance. The efficiency of the different methods strongly varies with the number of clusters and CDs selected using the different dimension reduction methods. On average, GC and KM appear to give the worst results since those methods perform worse than RE in every case. HC and RA yield the best results, while the performance of RE and RT is intermediate.

The probability of finding a better set of groups than RE (representing one group) is under 20% when creating two groups, and it goes below 5% in the case of four groups (Fig. 8.). Even the best performing RA reaches only the upper 10% of the CDF when creating two groups. In Table 3 we only provided the best performing set of CDs, but APR results in the list of best performing CD combinations. The authors found that when relying on the result of APR using one CD, the second best parameter, the catchment width (W) can be used to create both two and four clusters performing in the upper 1%. The optimal clusters found by the MC method and the groups created using W only are presented in Fig. 9. The catchment groups of the two methods differ; therefore, the connection between the catchments within a cluster resulting from the MC approach is not clear. However, the grouping based on W outperformed all other clustering methods with an *NSE* value of 0.693 and 0.697 as well as an *RMSE* value of 5.80 and 5.77 h, when creating two and four clusters, respectively.

4.3. Existing empirical equations

The four existing empirical equations performed worse than the derived new equations in general. The Haktanir-Shezen equation performed best in comparison with the equations including one CD (see Tables 2 and 3). However, even the equation created by using the result of PCA gave slightly better results. Interestingly and unfortunately, the most often applied Wisnovszky equation gave the worst results. Even the Salcher equation performed better, from which the former was derived. Wisnovszky's methodology to improve the performance of the Salcher equation was purely theoretical. He introduced a parameter describing catchment shape, which is similar to S_b. In fact, the Wisnovszky equation can be written as $T_c = \frac{L \cdot S_b^{0.5}}{(S/100)^{0.5}}$. Interestingly, the exponent of S_b (0.5) is very close to the one calibrated by the authors (0.46). However, instead of L and S, other CDs proved to be more efficient to estimate T_r. The Ventura equation's performance is between Wisnovszky's and Salcher's. The *NSE* value reaches 0.210 in the case of the Haktanir-Shezen equation. Compared to that, the *NSE* value of 0.583 resulting from the APR method (see Table 3), using three CDs (without clustering) is clearly a significant improvement. The error of the most often used Wisnovszky equation underlines the need for the new empirical equation.

5. Discussion and conclusions

The variety of the selected CDs in the different dimension-reduction methods is relatively wide, which underlines the need for comparative studies. From a hydraulic point of view, it is not surprising that L and S showed the strongest correlation with T_r. Also, these two CDs are very often used in empirical and semi-empirical equations (Nagy et al., 2016) primarily when they are derived from the Chezy equation, such as the equation used in Hungary (Wisnovszky, 1958). Another often used CD is the catchment area (A); however, it was not selected by any of the dimension reduction methods. Instead, P and A_g were selected, which are closely related to A. Three shape indices (R_c, C, and S_b) were also selected by the three dimension-reduction methods applied, which denotes the influence of catchment shape on response time. However, none of the hydro-climatological and channel network parameters were selected.

The most exciting result appeared to be the selection of fc_0 by APR, since it verifies the hydrological applicability of the 3D Soil Hydraulic Database of Europe (Toth et al., 2017). The inverse relationship between fc_0 and T_r is plausible, since a lower water retention capability can lead to a higher amount of groundwater recharge, therefore, a higher proportion of subsurface runoff. The latter can be attributed to a slower response time than that for surface runoff, verifying fc_0's influence on T_r. Following this reasoning, *BFI* could have been selected instead of fc_0 since its value should describe the same phenomenon. However, the calculated values of *BFI* do not necessarily represent the true values, since the exact amount of base flow is unknown.

It was shown that PCA in itself is not sufficient to select the best CDs to predict a hydrologic variable. Even the simple and arbitrary LCM method outperforms PCA, especially as the number of involved parameters grows. APR is computationally more expensive and requires more advanced programming skills but yields the absolute best set of parameters and the CDFs of estimation error. The shift in the CDFs does not imply a significant improvement in the model performance due to increasing the number of CDs involved in the calibrated equation. Therefore, the use of 2 or 3 CDs is suggested for catchment with similar climatic and geographic conditions.

The flattening of the CDFs in relation to the different number of groups applied clearly highlights the sensitivity of the derived equations to extrapolation. In the future, the applicability of fewer groups may be warranted. Based on the results related to the estimation of T_r, it is also questionable whether the use of six geographical regions is beneficial to estimate design flows in Hungary (General Directorate of Water Management, 2001). Considering the results of APR, the improvement in model performance is significant when two groups are created instead of one, but applying four groups instead of two does not yield a considerable change.

The performance of the different clustering methods is highly variable. There is no distinguishable clustering method that performs best amongst the employed dimension-reduction methods and group numbers. This underscores further the effect and significance of CD selection. KM and HC are often used for clustering and are easy to perform using the built-in functions, e.g., in MATLAB, but they perform inconsistently. RA is the only method that outperforms GC in most cases, but it does not always perform better than RE. The authors suggest using catchment width (W) combined with APR to estimate T_r for catchment groups. This method is the most likely to provide the best results in similar climatic and geographic conditions. However, the thresholds for W to differentiate between clusters

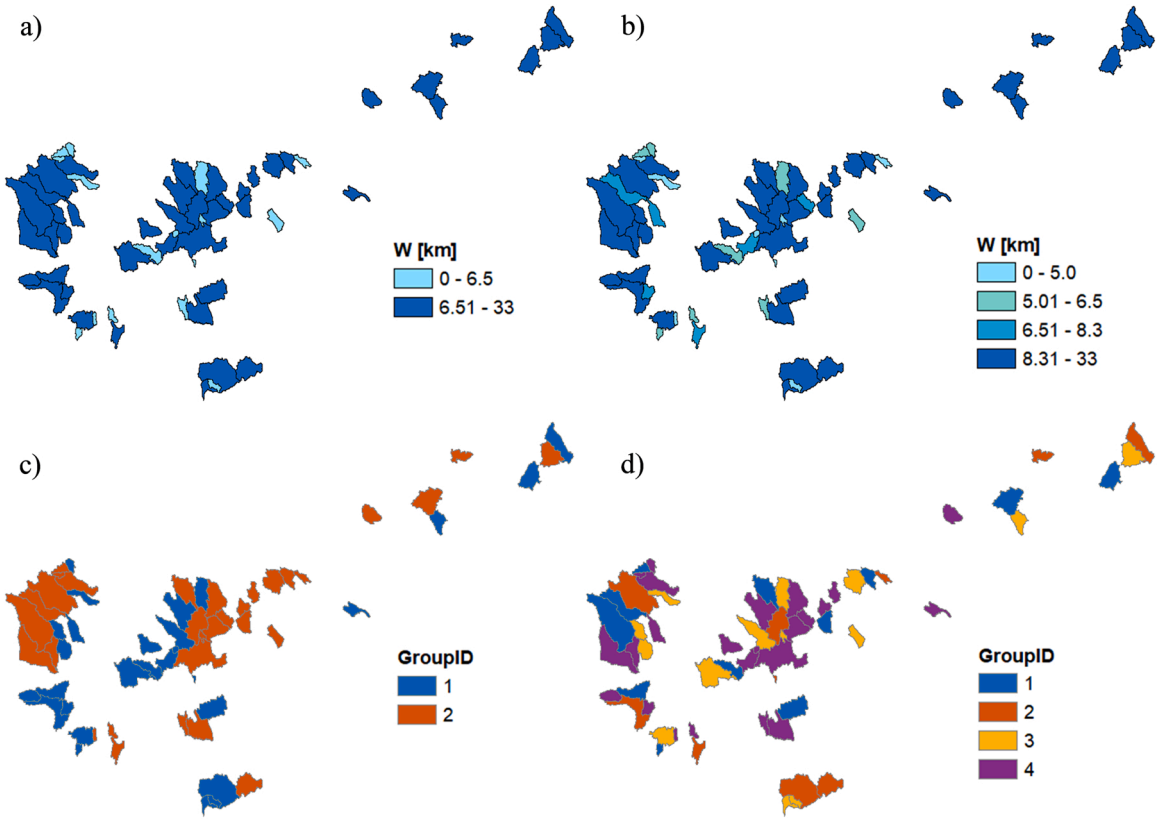

Fig. 9. The two and four groups created by employing catchment width (W) (a & b). The optimal two and four groups found by the MC approach (c & d).

[as presented in Fig. 9. a) & b)] may not yield similarly satisfactory results for a different set of catchments. The authors found it surprising that from the 60 more or less complex CDs, W appeared to provide a solid base to create catchment groups. Since W is related to both catchment size and shape, it is not unlikely that this result can be verified for another set of catchments.

As a summary, we collected 60 CDs for 61 Hungarian catchments, while calculating the characteristic, observed value of T_r. First, we compared eight different graphical definitions of T_r (Nagy and Szilágyi, 2020), then we applied the method of Giani et al. (2021) to calculate the value of T_r at the event scale. In this paper, we presented the outcome of a broad study involving three dimension reduction and seven clustering techniques, which yielded significantly more accurate empirical equations than the ones employed in Hungary. However, there are still many further possibilities in the research of relating T_r to catchment characteristics.

The efficiency of other clustering methods, such as Bayesian networks, as presented by Ssegane et al. (2012) and/or neural networks, should also be evaluated. As Ravazzani et al. (2019) state, the value of T_r is only weakly driven by climatological and morphological factors. Two approaches could deal with this problem: i) evaluating calculations based on hydraulic equations as in Beven (2020) or Michailidi et al. (2018), and; ii) employing a stochastic approach. The difficulty with the former approach is to set a proper value for the hydraulic parameters, such as roughness. The latter approach means that observed values could be employed to fit a theoretical distribution function. The parameters of the distribution can then be connected to catchment characteristics. The authors wish to evaluate both of these approaches in the future in order to further examine and explain the variability in the observed value of T_r, as illustrated in Fig. 3. Continuing the study presented in this paper this way will hopefully lead to a more detailed and accurate estimation of T_r.

CRediT authorship contribution statement

Eszter D. Nagy: Conceptualization, Methodology, Software, Formal analysis, Investigation, Data curation, Writing – original draft, Visualization. **Jozsef Szilagyi:** Writing – review & editing, Supervision. **Peter Torma:** Writing – review & editing, Supervision.

Declaration of Competing Interest

The authors declare that they have no known competing financial interests or personal relationships that could have appeared to influence the work reported in this paper.

Acknowledgments

This research, carried out at the Budapest University of Technology and Economics, was supported by the "TKP2020, Institutional Excellence Program" of the National Research, Development and Innovation (NRDI) Office in the field of Water Sciences and Disaster Prevention (BME IE-VIZ TKP2020). Partial support by the ÚNKP-20–3 new national excellence program of the Ministry for Innovation and Technology from the NRDI Fund as well as the data service of the local Water Directorates are also gratefully acknowledged. Finally, the authors would like to express their gratitude for the comments and suggestions provided by the reviewers.

Appendix A. List of geomorphological parameters

A1. Size and relief

Abbreviation	Name	Unit	Reference	Formula/Description
W	Basin width	km	Black (1972)	The length of the line perpendicular to the longest flow path, passing the center of the catchment area, extended to the catchment boundary.
L_c	Length from centroid to outlet	km	Black (1972)	The length of the line connecting the center of mass of the catchment area and the catchment outlet.
L_b	Basin length	km		The broken line's length, connecting the outlet point, the catchment centroid, and the end of the longest flow path.
P	Basin perimeter	km		
A	Basin area	km^2		
S	Slope of longest flow path	%		$S = \frac{H/1000}{L} \bullet 100$
S_a	Average slope of watershed	%		Average of the slope raster, calculated using the Slope tool from the ArcHydro Toolbox.
L	Longest flow path	km		Geometrically longest flow path, based on the DEM of the catchment (ArcHydro Toolbox/Longest Flow Path).
H_{min}	Minimum elevation	m a.s.l.		
H_{max}	Maximum elevation	m a.s.l.		
H_{mean}	Average elevation	m a.s.l.		
S_{ms}	Main stream channel slope	%		The average slope of the channel sections coinciding with the longest flow path.
H	Relief	m	Schumm (1956)	$H = H_{max} - H_{min}$
$R_{r,2}$	Relief ratio	%	Schumm (1956)	$R_{r,2} = \frac{H/1000}{L_b} \bullet 100$
$R_{r,1}$	Relative relief	%		$R_{r,1} = \frac{H/1000}{P} \bullet 100$
$R_{r,m}$	Melton relative relief	%	Melton (1965)	$R_{r,m} = \frac{H/1000}{\sqrt{A}} \bullet 100$
HI	Hypsometric integral	–	Pike and Wilson (1971)	$HI = \frac{H_{mean} - H_{min}}{H}$
D_i	Dissection index	–	Singh and Dubey (1994)	$D_i = \frac{H}{H_{max}}$
S_r	Slope ratio	–	Al-Rawas and Valeo (2010)	$S_r = \frac{S_{ms}}{S_a}$

A2. Topography

Abbreviation	Name	Unit	Reference	Formula/Description
A_u	Urban (impervious) area	%	Copernicus (2020b)	$A_u = \frac{a_u}{A} * 100$, where a_u was calculated as the sum of the cell values multiplied by the cell size.
A_f	Forested area	%	Copernicus (2020a)	$A_f = \frac{a_f}{A} * 100$, where a_f was calculated as the sum of the cell values multiplied by the cell size.
A_g	Grasslands	%		$A_g = 100 - (A_u + A_f)$
A_{karst}	Proportion of karst	%		
ths_0	Saturated water content	–	Toth et al. (2017)	Averaged value of the gridded data at the topmost level (0 cm).
fc_0	Field capacity	–	Toth et al. (2017)	Averaged value of the gridded data at the topmost level (0 cm).
ks_0	Saturated hydraulic conductivity	cm/day	Toth et al. (2017)	Averaged value of the gridded data at the topmost level (0 cm).
wp_0	Wilting point	–	Toth et al. (2017)	Averaged value of the gridded data at the topmost level (0 cm).

A3. Channel network

Abbreviation	Name	Unit	Reference	Formula/Description
SN	Total stream number	pcs		Number of channel segments, divided by junction point.
SL	Total stream length	km		The threshold for streams was 1 km^2 catchment area.
L_{max}	Length of main stream	km		Length of the channel sections coinciding with the longest flow path.
u	Highest stream order	–	Strahler (1957)	After Strahler's hierarchical stream ordering. L_u, N_u, and A_u are the length, number, and area belonging to the highest order of channels.
L_u	Main trunk length (highest stream order length)	km		
Sin	Sinuosity	–	Mueller (1968)	$Sin = \frac{L}{L_b}$
S_f	Stream frequency	1/ km^2	Horton (1945)	$S_f = \frac{SN}{A}$
D_d	Drainage density	1/ km	Horton (1932)	$D_d = \frac{SL}{A}$
D_f	Drainage factor	–		$D_f = \frac{S_f}{D_d^2}$
C_m	Channel maintenance	km	Schumm (1956)	$C_m = \frac{1}{D_d}$
L_o	Overland flow length	km	Horton (1945)	$L_o = \frac{1}{2 \bullet D_d}$
T	Drainage texture	1/ km	Smith (1950)	$T = D_d \bullet \mathrm{D_f}$
R_t	Texture ratio	1/ km	Smith (1950)	$R_t = \frac{SN}{P}$
R_f	Fineness ratio	–	Melton (1965)	$R_f = \frac{SL}{P}$
R_b	Bifurcation ratio	–	Singh and Yousuf (2000)	$R_b = \frac{N_u}{N_{u-1}}$
R_l	Stream length ratio	–	Singh and Yousuf (2000)	$R_l = \frac{L_u}{L_{u-1}}$
R_a	Area ratio	–	Horton (1932)	$R_a = \frac{A_u}{A_{u-1}}$

A4. Shape indices

Abbreviation	Name	Unit	Reference	Formula/Description
L_{sc}	Distance from stream centroid	km		The length of the line perpendicular to the longest flow path going to the centroid of the catchment.
R_c	Elongation ratio	–	Schumm (1956)	$R_c = \frac{2 \bullet \sqrt{A/\pi}}{L_b}$
S_b	Basin shape factor	–		$S_b = \frac{L^2}{A}$
R_{lw}	Length-width ratio	–		$R_{lw} = \frac{L}{W}$
C	Compactness	–	Horton (1932)	$C = \frac{P}{2 \bullet \sqrt{\pi \bullet A}}$
c	Basin circularity	–	Miller (1953)	$c = \frac{4 \bullet \pi \bullet A}{P^2 =} \frac{1}{C^2}$
F	Form factor	–	Horton (1932)	$F = \frac{A}{L_b^2}$
K	Lemniscate ratio	–	Chorley et al. (1957)	$K = \frac{L_b^2 \bullet \pi}{4 \bullet A}$
t	Eccentricity	–	Black (1972)	$t = \frac{\sqrt{\lvert L_C^2 - W^2 \rvert}}{W}$
RN	Ruggedness number	–		$R_N = \frac{H \bullet D_d}{1000}$
CON	Contiguity index	–	Lagro (1991)	$CON_{ij} = \frac{\frac{\sum_{r=1}^{z} C_{ijr}}{a_{ij}} - 1}{v - 1}$ A detailed description of the variables can be found in Lagro (1991). The contiguity of land use patches was calculated, using the main categories (1–5) of the Corine Land Cover maps.

A5. Hydro-climatological indices

Abbreviation	Name	Unit	Reference	Formula/Description
MAR	Mean annual runoff	mm		Long-term average of the total annual runoff for the period of record.
MAP	Mean annual precipitation	mm		Long-term average of the total annual precipitation for the period of record.
α	Runoff ratio	–		$\alpha = \frac{MAR}{MAP}$
BFI	Base flow index	–		Ratio of base flow and total flow for the period of record.
FI	Flashiness index	–	Baker et al. (2004)	$FI = \sum_{i=1}^{N} \frac{\sum_{j=1}^{n} \left\lvert q_{i,j} - q_{i,j-1} \right\rvert}{\sum_{j=1}^{n} q_{i,j}} / N$, where N is the number of years, $n = 365(366)$, and q is the daily mean discharge.

Appendix B. Supporting information

Supplementary data associated with this article can be found in the online version at doi:10.1016/j.ejrh.2021.100971.

References

Al-Rawas, G.A., Valeo, C., 2010. Relationship between wadi drainage characteristics and peak-flood flows in arid northern Oman. Hydrol. Sci. J. 55 (3), 377–393. https://doi.org/10.1080/02626661003718318.

Azizian, A., 2018. Uncertainty analysis of time of concentration equations based on first-order-analysis (FOA) method. Am. J. Eng. Appl. Sci. 11 (1), 327–341. https://doi.org/10.3844/ajeassp.2018.327.341.

Baker, D.B., Richards, P.R., Loftus, T.T., Kramer, J.W., 2004. A new flashiness index: characteristics and applications to Midwestern Rivers and streams. J. Am. Water Resour. Assoc. 4, 503–522.

Beven, K.J., 2020. A history of the concept of time of concentration. Hydrol. Earth System Sci. 24, 2655–2670. https://doi.org/10.5194/hess-24-2655-2020.

Black, P.E., 1972. Hydrograph response to geomorphic model watershed characteristics and precipitation variables. J. Hydrol. 17 (4), 309–329. https://doi.org/10.1016/0022-1694(72)90090-X.

Blöschl, G., Sivapalan, M., Wagener, T., Viglione, A., Savenije, H., 2013. Runoff Prediction in Ungauged Basins. Cambridge University Press, New York. https://doi.org/10.1017/CBO9781139235761.

Boscarello, L., Ravazzani, G., Cislaghi, A., Mancini, M., 2016. Regionalization of flow-duration curves through catchment classification with streamflow signatures and physiographic-climate indices. J. Hydrol. Eng. 21 (3), 05015027. https://doi.org/10.1061/(ASCE)HE.1943-5584.0001307.

Breiman, L., Friedman, J.H., Olshen, R.A., Stone, C.J., 1984. Classification and Regression Trees. Wadsworth International Group, Belmont.

Chorley, R.J., Malm, D.E.G., Pogorzelski, H.A., 1957. A new standard for estimating drainage basin shape. Am. J. Sci. 255 (2), 138–141. https://doi.org/10.2475/ajs.255.2.138.

Copernicus, L.M.S., 2016. European Digital Elevation Model (EU-DEM), version 1.1. ⟨https://land.copernicus.eu/imagery-%20in-situ/eu-dem/eu-dem-v1.1⟩ (Accessed 14 July 2019).

Copernicus, L.M.S., 2020a. Tree Cover Density 2018. ⟨https://land.copernicus.eu/pan-european/high-resolution-layers/forests/tree-cover-density/status-maps/tree-cover-density-2018⟩ (Accessed 5 September 2020).

Copernicus, L.M.S., 2020b. Imperviousness Density 2018. ⟨https://land.copernicus.eu/pan-european/high-resolution-layers/imperviousness/status-maps/imperviousness-density-2018⟩ (Accessed 5 September 2020).

Copernicus Climate Change Service (C3S), 2019. C3S ERA5-Land Reanalysis. Copernicus Climate Change Service,, 2019.08.16.

Everitt, B.S., Landau, S., Leese, M., Stahl, D., 2011. Cluster Analysis. King's College London. Wiley. https://doi.org/10.1007/BF00154794.

Fang, X., Thompson, D.B., Cleveland, T.G., Pradhan, P., Malla, R., 2008. Time of concentration estimated using watershed parameters determined by automated and manual methods. J. Irrig. Drain. Eng. 134 (2), 202–211. https://doi.org/10.1061/(ASCE)0733-9437(2008)134:2(202).

Fox, J., 2016. Applied Regressions Analysis and Generalized Linear models. SAGE Publications.

Gaál, L., Szolgay, J., Kohnová, S., Parajka, J., Merz, R., Viglione, A., Blöschl, G., 2012. Flood timescales: understanding the interplay of climate and catchment processes through comparative hydrology. Water Resour. Res. 48 (4) https://doi.org/10.1029/2011WR011509.

General Directorate of Water Management , 2001. Manual on Design Flow Estimation (in Hungarian). Budapest.

Giani, G., Rico-Ramirez, M.A., Woods, R.A., 2021. A practical, objective, and robust technique to directly estimate catchment response time. Water Resour. Res. 57 (2) https://doi.org/10.1029/2020WR028201.

Grimaldi, S., Petroselli, A., Tauro, F., Porfiri, M., 2012. Time of concentration: a paradox in modern hydrology. Hydrol. Sci. J. 57 (2), 217–228. https://doi.org/10.1080/02626667.2011.644244.

Gugel, H.W., 1972. SELECT-A Computer Program for Isolating "Best" Regressions. General Motor Corp. Res. Pub.

Haktanir, T., Sezen, N., 1990. Suitability of two-parameter gamma and three-parameter beta distributions as synthetic unit hydrographs. Hydrol. Sci. J. 35 (2), 167–184. https://doi.org/10.1080/02626669009492416.

Hocking, R.R., 1976. A biometrics invited paper. the analysis and selection of variables in linear regression. Biometrics 32 (1), 1. https://doi.org/10.2307/2529336.

Horton, R.E., 1932. Drainage-basin characteristics. Eos Trans. Am. Geophys. Union 13 (1), 350–361. https://doi.org/10.1029/TR013i001p00350.

Horton, R.E., 1945. Erosional development of streams and their drainage basins; hydrophysical approach to quantitative morphology. GSA Bull. 56 (3), 275–370. https://doi.org/10.1130/0016-7606(1945)56[275:EDOSAT]2.0.CO;2.

Kaufmann de Almeida, I., Kaufmann Almeida, A., Garcia Gabas, S., Alves Sobrinho, T., 2017. Performance of methods for estimating the time of concentration in a watershed of a tropical region. Hydrol. Sci. J. 62 (14), 2406–2414. https://doi.org/10.1080/02626667.2017.1384549.

Laaha, G., Blöschl, G., 2006. A comparison of low flow regionalisation methods-catchment grouping. J. Hydrol. 323 (1–4), 193–214. https://doi.org/10.1016/j.jhydrol.2005.09.001.

Lagro, J., 1991. Assessing patch shape in landscape mosaics. Photogramm. Eng. Remote Sens. 57 (3), 285–293.

Lloyd, S.P. , 1982. Least Squares Quantization in PCM. IEEE Transactions on Information Theory, 28(2), 129–137. https://doi.org/10.1109/TIT.1982.1056489.

McCuen, R.H., Wong, S.L., Rawls, W.J., 1987. Estimating urban time of concentration. J. Hydraul. Eng. 113 (1), 127–128. https://doi.org/10.1061/(ASCE)0733-9429(1987)113:1(127).

Melton, M.A., 1965. The geomorphic and paleoclimatic significance of alluvial deposits in Southern Arizona. J. Geol. 73 (1), 1–38. https://doi.org/10.1086/627044.

Michailidi, E.M., Antoniadi, S., Koukouvinos, A., Bacchi, B., Efstratiadis, A., 2018. Timing the time of concentration: shedding light on a paradox. Hydrol. Sci. J. 63 (5), 721–740. https://doi.org/10.1080/02626667.2018.1450985.

Miller, V.C., 1953. A Quantitative Geomorphic Study of Drainage Basin Characteristics in the Clinch Mountain Area, Virginia and Tennessee. Department of Geology. Columbia University.
Mueller, J.E., 1968. An introduction to the hydraulic and topographic sinousity indexes. Ann. Assoc. Am. Geogr. 58 (2), 371–385. https://doi.org/10.1111/j.1467-8306.1968.tb00650.x.
Myronidis, D., Ivanova, E., 2020. Generating regional models for estimating the peak flows and environmental flows magnitude for the bulgarian-greek rhodope mountain range torrentialwatersheds. Water 12 (3). https://doi.org/10.3390/w12030784.
Nagy E.D. , Szilágyi J. , Comparative analysis of catchment response times and their definitions using measured and reanalysis rainfall data HydroCarpath International Conference: Processes, Patterns and Regimes in the Hydrology of the Carpathians: Coupling Experiments, Remote Sensing, Citizen Science 9 2020 doi: 10.13140/RG.2.2.29763.02089.
Nagy, E.D., Torma, P., Bene, K., 2016. Comparing methods for computing the time of concentration in a medium-sized Hungarian catchment. Slovak J. Civil Eng. 24 (4), 8–14. https://doi.org/10.1515/sjce-2016-0017.
Nash, J.E., Sutcliffe, J.V., 1970. River flow forecasting through conceptual models part I – a discussion of principles. J. Hydrol. 10 (3), 282–290. https://doi.org/10.1016/0022-1694(70)90255-6.
Parajka, J., Merz, R., Blöschl, G., 2005. A comparison of regionalisation methods for catchment model parameters. Hydrol. Earth System Sci. 9, 157–171. https://doi.org/10.5194/hess-9-157-2005.
Peel, M.C., Finlayson, B.L., Mcmahon, T.A., 2007. Updated world map of the Köppen-Geiger climate classification. Hydrol. Earth System Sci. 11, 1633–1644. https://doi.org/10.5194/hess-11-1633-2007.
Perdikaris, J., Gharabaghi, B., Rudra, R., 2018. Reference time of concentration estimation for ungauged catchments. Earth Sci. Res. 7 (2), 58–73. https://doi.org/10.5539/esr.v7n2p58.
Pike, R.J., Wilson, S.E., 1971. Elevation-relief ratio, hypsometric integral, and geomorphic area-altitude analysis. GSA Bull. 82 (4), 1079–1084. https://doi.org/10.1130/0016-7606(1971)82[1079:ERHIAG]2.0.CO;2.
Pilgrim, D.H., 1976. Travel times and nonlinearity of flood runoff from tracer measurements on a small watershed. Water Resour. Res. 12 (3), 487–496. https://doi.org/10.1029/WR012i003p00487.
Ravazzani, G., Boscarello, L., Cislaghi, A., Mancini, M., 2019. Review of time-of-concentration equations and a new proposal in Italy. J. Hydrol. Eng. 24 (10), 1–11. https://doi.org/10.1061/(ASCE)HE.1943-5584.0001818.
Sanborn, S.C., Bledsoe, B.P., 2006. Predicting streamflow regime metrics for ungauged streamsin Colorado, Washington, and Oregon. J. Hydrol. 325 (1–4), 241–261. https://doi.org/10.1016/j.jhydrol.2005.10.018.
Sauquet, E., Catalogne, C., 2011. Comparison of catchment grouping methods for flow duration curve estimation at ungauged sites in France. Hydrol. Earth System Sciences 15, 2421–2435. https://doi.org/10.5194/hess-15-2421-2011.
Schumm, S.A., 1956. Evolution of drainage systems and slopes in badlands at Perth Amboy, New Jersey. GSA Bull. 67 (5), 597–646. https://doi.org/10.1130/0016-7606(1956)67[597:EODSAS]2.0.CO;2.
Singh, S., Dubey, A.,1994. Geoenvironmental planning of watersheds in India.
Singh, P.K., Kumar, V., Purohit, R.C., Kothari, M., Dashora, P.K., Kumar, V., Kothari, M., 2009. Application of principal component analysis in grouping geomorphic parameters for hydrologic modeling. Water Resour. Manag. 23, 325–339. https://doi.org/10.1007/s11269-008-9277-1.
Singh, M., Yousuf, A., 2000. Watershed Hydrology, Management and Modeling. CRC Press.
Smith, K.G., 1950. Standards for grading texture of erosional topography. Am. J. Sci. 248 (9), 655–668. https://doi.org/10.2475/ajs.248.9.655.
Ssegane, H., Tollner, E.W., Mohamoud, Y.M., Rasmussen, T.C., Dowd, J.F., 2012. Advances in variable selection methods I: Causal selection methods versus stepwise regression and principal component analysis on data of known and unknown functional relationships. J. Hydrol. 438–439, 16–25. https://doi.org/10.1016/j.jhydrol.2012.01.008.
Strahler, A.N., 1957. Quantitative analysis of watershed geomorphology. Eos Trans. Am. Geophys. Union 38 (6), 913–920. https://doi.org/10.1029/TR038i006p00913.
Toth, B., Weynants, M., Pasztor, L., Hengl, T., 2017. 3D soil hydraulic database of Europe at 250 m resolution. Hydrol. Process. 31 (14), 2662–2666. https://doi.org/10.1002/hyp.11203.
Wisnovszky, I., 1958. The computation of the time of concentration (in Hungarian). Hung. J. Hydrol. 3, 195–200.